Draft version March 19, 2022
Preprint typeset using LaTeX style emulateapj v. 14/09/00

arXiv:astro-ph/0111158v2 31 Mar 2002

RELIABILITY OF THE DARK MATTER CLUSTERING IN COSMOLOGICAL N-BODY SIMULATION ON SCALES BELOW THE MEAN SEPARATION LENGTH OF PARTICLES

Takashi Hamana[1,2], Naoki Yoshida[2,3], and Yasushi Suto[4]
[1]National Astronomical Observatory, Mitaka 181-8588, Japan
[2]Max-Planck-Institut für Astrophysik, Karl-Schwarzschild-Strasse 1, 85748 Garching, Germany
[3]Harvard-Smithsonian Center for Astrophysics 60 Garden Street, Cambridge MA02138
[4]Department of Physics and Research Center for the Early Universe (RESCEU)
School of Science, University of Tokyo, Tokyo 113-0033, Japan
hamana@yukawa.kyoto-u.ac.jp, nyoshida@cfa.harvard.edu, suto@phys.s.u-tokyo.ac.jp
Draft version March 19, 2022

ABSTRACT

We critically examine the reliability of the dark matter clustering in high-resolution cosmological N-body simulations on scales below the mean separation length of particles. The particle discreteness effect imposes the two fundamental limitations on those scales; the lack of the initial fluctuation power and the finite mass resolution. We address this problem applying the dark halo approach and are able to discuss separately how those two limitations affect the dark matter clustering in N-body simulations at early epochs. We find that limitations of the dark matter clustering are primarily determined by the mass of particles. By a detailed comparison with three major cosmological simulations, we also find that in order to reproduce a proper amplitude of the dark matter clustering on small scales, halos with a characteristic nonlinear mass, $M_{\rm NL}(z)$ defined by $\sigma_R(M_{\rm NL};z)=1$, must be resolved in the simulation. This leads to a critical redshift $z_{\rm crit}$ determined by $M_{\rm NL}(z_{\rm crit})=n_{\rm halo}m_{\rm part}$ where $n_{\rm halo}$ is the number of particles necessary to resolve the typical nonlinear mass halo (~ 10). We conclude that, at least as far as the two-point correlation functions are concerned, the dark matter clustering in high-resolution N-body simulations on scales below the mean particle separation is reliable down to the gravitational force resolution length only for $z<z_{\rm crit}$, while it is strongly affected by the finite mass resolution for $z>z_{\rm crit}$.

Subject headings: gravitation — cosmology: theory – dark matter – large-scale structure of universe – methods: N-body simulations

1. INTRODUCTION

N-body simulations have played a key role in studying large-scale structure formation in the universe. In particular, they enable one to probe the quasi-linear to nonlinear clustering in a direct manner without resorting to any unrealistic approximations. Thus they are extensively used in cosmology as a powerful and indispensable tool complementary to analytical techniques. Cosmological N-body simulations have been first applied in exploring the nonlinear growth of two-point correlation functions (Miyoshi & Kihara 1975; Aarseth, Gott, & Turner 1979), and in studying the halo mass function (Press & Schechter 1974). A seminal paper by Davis et al. (1985) clearly demonstrated that this methodology provides a variety of testable predictions for a given cosmological model. Since then almost all precise predictions in gravitational nonlinear phenomena have relied heavily on N-body simulations, including accurate nonlinear modeling of the dark matter power spectrum (Hamilton et al. 1991; Peacock & Dodds 1996), redshift-space distortion (Suto & Suginohara 1991; Cole, Fisher & Weinberg 1994; Magira, Jing & Suto 2000), three- and four-point correlation functions (Suto 1993; Matsubara & Suto 1994; Suto & Matsubara 1994), probability distribution function of the nonlinear density field (Suto, Itoh & Inagaki 1990; Lahav et al. 1993; Kayo, Taruya & Suto 2001), the mass function of virialized dark halos (Bahcall & Cen 1993; Sheth & Tormen 1999; Jenkins et al. 2001), the density profiles of dark matter halos (Navarro, Frenk & White 1996,1997; Fukushige & Makino 1997; Moore et al. 1998; Jing & Suto 2000; Yoshida et al. 2000), dark halo biasing (Watanabe, Matsubara, & Suto 1994; Jing & Suto 1998; Jing 1998; Sheth & Tormen 1999; Colberg et al. 2000; Taruya et al. 2001), and clustering on the past light-cone (Hamana et al. 2001a,b; Evrard et al. 2001).

Of course, the reliability of N-body simulations is severely limited by various numerical restrictions. Among them, the effective dynamical range is quite important. Consider a simulation employing $N_{\rm part}$ particles in a comoving cubic box of $L_{\rm box}^3$. Obviously the *mass resolution* is set by the number of particles, and the corresponding resolution in length scale is up to the mean particle separation $\lambda_{\rm part}=L_{\rm box}/N_{\rm part}^{1/3}$. In fact, the initial perturbations of simulations are usually set on uniform grid points of an interval $\lambda_{\rm part}$. Therefore one cannot properly set the desired initial power spectrum for $k>k_{\rm Nyquist}$ where $k_{\rm Nyquist}=\pi/\lambda_{\rm part}$ is the Nyquist wavenumber[1]. Nevertheless most N-body codes adopt a *force resolution* (e.g., the gravitational softening length $\epsilon_{\rm grav}$) typically one order of magnitude smaller than $\lambda_{\rm part}$. Are these *high-resolution*

[1] This is also the case for a N-body simulation that adopts a "glass" distribution for particles to represent an initial uniform state (White 1996, Jenkins et al. 1998), because the Nyquist wavenumber in this case is also set by $k_{\rm Nyquist}=\pi/\lambda_{\rm part}$.

[2] Throughout the present paper, we use the term "high-resolution simulation" to refer to the N-body codes that employ the gravitational

simulations [2] really reliable on scales below the particle mean separation length $\lambda_{\rm part}$ where the initial conditions cannot be set properly ? Although several attempts have been made to this direction (e.g., Efstathiou et al. 1985; 1988; Gelb & Bertschinger 1994; Melott et al. 1997; Splinter et al. 1998), this natural question has remained unanswered in a quantitative manner, and is exactly what we address in detail in the rest of the paper.

Qualitatively speaking, high-resolution simulations are justified *only if almost all the power on scales below the mean separation $\lambda_{\rm part}$ at later epochs is generated via nonlinear mode-coupling from the power on larger scales.* The transfer of the fluctuation power in cosmology due to the nonlinear mode-coupling is examined numerically by Suginohara et al. (1991), as well as by perturbation analysis in Suto & Sasaki (1991) and Makino, Sasaki & Suto (1992). According to their results, the nonlinear power transfer is expected to *eventually* dominate the initial power if the effective spectral index at the scale, $n_{\rm eff} \equiv d\log P(k)/d\log k$, is much less than -1. Actually this is indeed the case for most realistic cosmological scenarios including cold dark matter (CDM) models whose power spectrum asymptotically approaches $\propto k^{-3}$. Nevertheless the above qualitative argument does not answer precisely *when* the results below $\lambda_{\rm part}$ become reliable.

To be more specific, we examine the evolution of dark matter clustering in high-resolution cosmological N-body simulations taking explicit account of the two fundamental limitations: (i) the lack of the initial fluctuation power on scales smaller than the mean particle separation, and (ii) the finite mass resolution. To do this, we apply the dark halo approach in which the nonlinear dark matter two-point correlation function is described by a sum of two contributions; one from the correlations between the halos (halo-halo correlation), and the other from correlations of matter within the same halo (the Poisson contribution) (Peebles 1980 and references therein, for recent developments in the dark halo approach, see Ma & Fry 2000; Seljak 2000). We show in the following sections that this approach provides a simple but powerful way to examine separately how those two limitations affect the simulation results. This approach is quite different from previous ones which usually attempted to find convergence among different N-body codes with different numerical resolutions (e.g., Efstathiou et al. 1985, 1988; Gelb & Bertschinger 1994; Melott et al. 1997; Splinter et al. 1998; Moore et al. 1998; Jenkins et al. 1998, 2001; Knebe et al. 2000).

We focus on the two-point correlation function of dark matter to examine the limitations in high-resolution N-body simulations for the following reasons. Firstly, the two-point correlation function is one of the most fundamental statistics to quantify clustering properties, and has been studied in detail both analytically and numerically. Actually, there exist accurate fitting formulae of the dark matter power spectrum (Hamilton et al. 1991; Peacock & Dodds 1996) that reproduce the behavior of the two-point correlation function in linear to highly nonlinear regimes. Secondly, the estimator of the two-point correlation function from the particle distribution in N-body data is well established (Kerscher, Szapudi & Szalay 2000 and references therein). These two advantages enable us to investigate limitations in high-resolution N-body simulations through detailed comparison between numerical results and model predictions.

The outline of this paper is as follows. In §2, we summarize our dark halo approach, and demonstrate the extent to which the two limitations may affect the evolution of dark matter clustering on scales below the mean particle separation length. We present detailed comparison between a high-resolution N-body data and our model predictions in §3, and show that our model reproduces well an apparent depression in the dark matter two-point correlation function measured from those simulation data. In particular we find that the depression becomes less appreciable as the ratio of the characteristic nonlinear mass $M_{\rm NL}$ to the particle mass $m_{\rm part}$ increases. On the basis of this, we evaluate the critical redshift $z_{\rm crit}$ beyond which the correlation function of the dark matter in high-resolution N-body simulations on scales below the mean particle separation length suffers significantly from discreteness limitations. Finally §4 is devoted to a summary and further discussion.

2. DARK HALO APPROACH

The dark halo approach has a long history (Neyman & Scott 1952; Limber 1953; Peebles 1974, 1980; McClelland & Silk 1977), and has recently applied to various problems in galaxy formation and cosmological nonlinear clustering (Scherrer & Bertschinger 1991; White & Frenk 1991; Kauffmann, White & Guiderdoni 1993; Cole et al. 1994; Sheth & Jain 1997; Komatsu & Kitayama 1999; Somerville & Primack 1999; Seljak 2000; Peacock & Smith 2000; Ma & Fry 2000; Cooray, Hu & Miralda-Escude 2000; Cooray & Hu 2001). In this section, we summarize several expressions which are most relevant to the current analysis. Further details of this approach can be found in those papers.

2.1. *Ingredients in model predictions*

The accurate description of the matter clustering on the basis of the dark halo approach requires three major ingredients; the mass function of dark halos, the mass-dependent biasing factor of halos, and the density profile of halos. We present a summary of those three ingredients below.

We adopt an analytical model of the halo mass function proposed by Sheth & Tormen (1999):

$$\frac{dn}{dM}dM = \frac{\bar{\rho}_0}{M} f(\nu) d\nu = \frac{\bar{\rho}_0}{M} A[1+(a\nu)^{-p}]\sqrt{a\nu}\exp\left(-\frac{a\nu}{2}\right)\frac{d\nu}{\nu}, \quad (1)$$

where

$$\nu = \left[\frac{\delta_c(z)}{\sigma(M,z)}\right]^2, \quad (2)$$

$\bar{\rho}_0$ is the mean cosmic mass density, and the numerical coefficients a and p are empirically fitted from N-body simulations as $a = 0.707$ and $p = 0.3$. Here $\sigma(M,z)$ is the root-mean-square fluctuations in the matter density top-hat smoothed over a scale $R_M \equiv (3M/4\pi\bar{\rho}_0)^{1/3}$ and $\delta_c(z)$ is the threshold over-density for spherical collapse

[2] softening length smaller than the mean particle separation such as P^3M and Tree codes.

(see Nakamura & Suto 1997 and Henry 2000 for useful fitting functions). The normalization constant A in equation (1) is determined by requiring that

$$\frac{1}{\bar{\rho}_0}\int \frac{dn}{dM} M dM = \int f(\nu) d\nu = 1. \tag{3}$$

A simple analytic model of the halo bias was proposed by Mo & White (1996) applying the extended Press-Schechter theory (e.g., Lacey & Cole 1993). Jing (1998) and Sheth & Tormen (1999) discussed the correction for the mass-dependence, and the stochastic nature of the halo biasing is considered subsequently by Taruya & Suto (2000) and Somerville et al. (2001). For the present purpose, we use the scale-independent model by Sheth & Tormen (1999) which reasonably reproduces N-body data:

$$b(\nu) = 1 + \frac{a\nu - 1}{\delta_c} + \frac{2p}{\delta_c(1+a\nu)}. \tag{4}$$

Finally we have to specify the density profile of dark matter halos. We adopt the NFW profile (Navarro, Frenk & White 1996):

$$\rho(r) = \frac{\rho_s}{(r/r_s)(1+r/r_s)^2}, \tag{5}$$

where ρ_s and r_s denote the scaling density and radius. While more recent simulations (Fukushige & Makino 1997; Moore et al. 1998) suggest that the inner profile is indeed steeper, we adopt the original profile just for simplicity. It is conventional to introduce the concentration parameter $c = r_{\rm vir}/r_s$, where $r_{\rm vir}$ is the virial radius of the halo. In terms of this, the mass of halo is written as

$$M = \frac{4\pi\rho_s r_{\rm vir}^3}{c^3}\left[\log(1+c) - \frac{c}{1+c}\right]. \tag{6}$$

Since the spherical collapse model indicates that $M = 4\pi r_{\rm vir}^3 \delta_{\rm vir}(z)\bar{\rho}_0/3$ with $\delta_{\rm vir}(z)$ being the over-density of collapse (see, Nakamura & Suto 1997; Henry 2000), one can express ρ_s in terms of M and c using equation (6). Thus our description of dark halos is completed if the concentration parameter c is expressed as a function of M and z. We adopt the following empirical relations:

$$c(M,z) = \begin{cases} \dfrac{8}{1+z}\left(\dfrac{M}{10^{14}h^{-1}M_\odot}\right)^{-0.13} & \text{for } \Lambda\text{CDM}, \\ \dfrac{5}{1+z}\left(\dfrac{M}{10^{14}h^{-1}M_\odot}\right)^{-0.13} & \text{for SCDM}. \end{cases} \tag{7}$$

The above c-M relation for ΛCDM model is suggested by Bullock et al. (2001), while for SCDM model, we adopt the smaller normalization found by Bartelmann et al. (1998). For simplicity, we do not take into account the scatter in c-M relation (Bullock et al. 2001), but it should have only secondary importance on a statistical measurement such like the two-point correlation function of the dark matter. We compare the dark matter power spectrum predicted by the dark halo approach (see next subsection) with that computed by the nonlinear fitting formula of Peacock & Dodds (1996). We find a good agreement between them for the SCDM and ΛCDM models over the range $0.01 < k[h{\rm Mpc}^{-1}] < 100$ and over $0 < z < 5$.

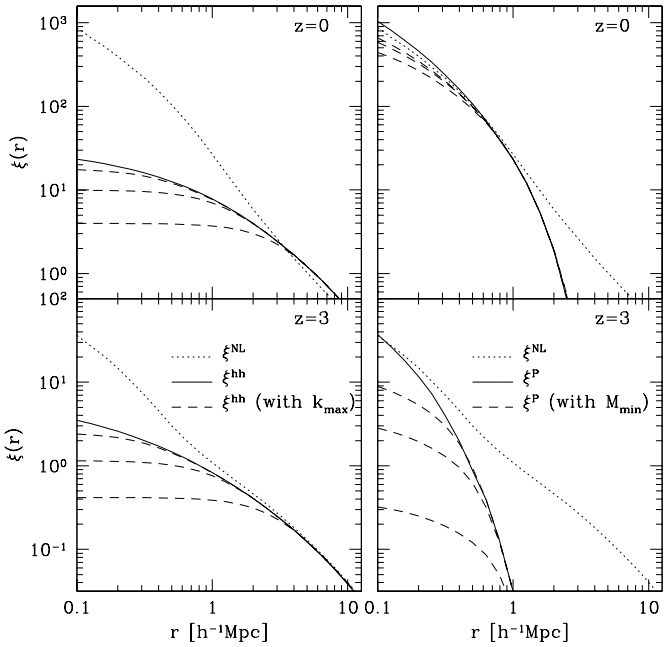


FIG. 1.— Comparison between dark matter two-point correlation functions predicted from the dark halo approach with and without taking into account the two limitations in the N-body simulation. *Left panels:* The effect of the lack of the initial perturbation power on small scales is demonstrated. The dotted line shows the nonlinear correlation function computed using Peacock & Dodds (1996) fitting function. The solid line shows the two-point correlation function from the halo-halo contribution without taking into account the small-scale cutoff, while the dashed lines from upper to lower are for $R_{\rm min} = 2\pi/k_{\rm max} = 0.3,\ 1,\ 3h^{-1}$Mpc. Top and bottom panels are for $z = 0$ and $z = 3$, respectively. *Right panels:* The effect of the finite mass resolution is demonstrated. The solid line shows the correlation function from the Poisson contribution in the case of no low mass cutoff, while the dashed lines from upper to lower are for $M_{\rm min} = 1,\ 3,\ 10\times10^{11}h^{-1}M_\odot$.

2.2. *Predicting two-point correlation functions*

In the dark halo approach, the two-point correlation function of the dark matter is the sum of two contributions; $\xi(r) = \xi^{\rm hh}(r) + \xi^{\rm P}(r)$. The first term ("the halo-halo contribution") arises due to the correlation between two halos of density profile $\rho(r)$ that are biased tracers of the dark matter distribution. In Fourier space, this term can be explicitly written as (Seljak 2000):

$$P^{\rm hh}(k) = P_{\rm lin}(k)\left[\int d\nu\, f(\nu) b(\nu) y(k;M)\right]^2, \tag{8}$$

where $P_{\rm lin}(k)$ is the linear power spectrum, $y(k;M)$ is the Fourier transform of the halo profile normalized by its mass, $y(k;M) = \tilde{\rho}(k,M)/M$, and M is related to ν via equation (2). The second "Poisson term" is due to the correlation between dark matter particles in the same halo and is expressed as

$$P^{\rm P}(k) = \int d\nu\, f(\nu)\frac{M(\nu)}{\bar{\rho}_0}|y(k;M)|^2. \tag{9}$$

Then the dark matter two-point correlation function is simply given by the sum of two terms

$$\xi^X(r) = \frac{1}{2\pi^2}\int dk\, k^2 \left[\frac{\sin(kr)}{kr}\right] P^X(k), \tag{10}$$

where X stands for either hh or P for the halo-halo and Poisson terms, respectively.

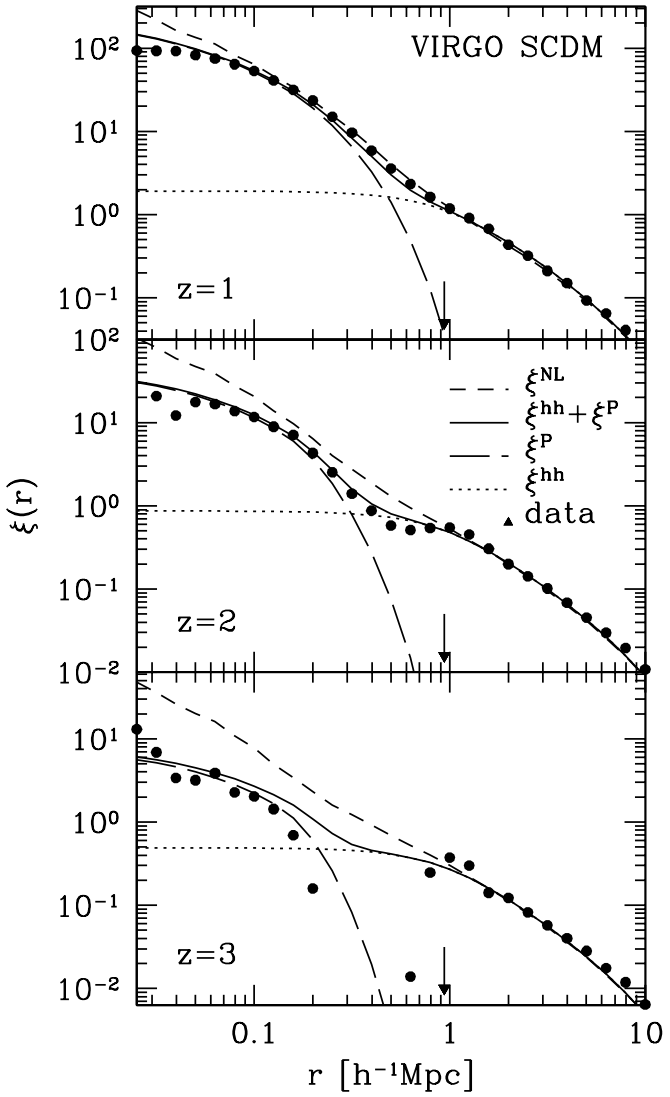


FIG. 2.— The two-point correlation function measured from the Virgo SCDM N-body simulation (filled circles) are compared with predictions. Dashed lines shows the nonlinear prediction by Peacock & Dodds (1996). Predictions by the dark halo approach, to which corrections for the lack of small-scale perturbation power and the finite particle mass are made (see §2), are shown by dotted, long-dashed and solid lines for the halo-halo term, Poisson term and their sum, respectively. The arrows indicate the mean separation lengths $\lambda_{\rm part}$ of simulation particles. The redshift of the realization is indicated in each panel.

2.3. *Effects of the lack of small-scale power and the finite mass resolution*

Before presenting the detailed comparison between simulations and our model predictions, it is instructive to show the main features that we expect in the present methodology. Figure 1 plots the dark matter two-point correlation functions at $z = 0$ (*Upper panels*) and $z = 3$ (*Lower panels*) for the set of parameters employed for the Virgo ΛCDM simulation (see Table 1). Solid lines in the left and right panels show the halo-halo and the Poisson terms, respectively. For comparison, dotted lines indicate the full nonlinear two-point correlation functions of the dark matter computed with the Peacock & Dodds (1996) formula. Clearly the large-scale power is well described by the halo-halo contribution only, while the small-scale power is dominated by the Poisson contribution.

To simulate the effect of the numerical limitations more quantitatively, we artificially set

$$P^{\rm hh}(k) = 0 \quad \text{for} \quad k > k_{\rm max} \tag{11}$$

for the halo-halo term, and

$$\frac{dn}{dM} = 0 \quad \text{for} \quad M < M_{\rm min} \tag{12}$$

for the Poisson term. The latter is equivalent to integrating equation (9) only for $\nu > \nu_{\rm min} \equiv [\delta_c(z)/\sigma(M_{\rm min}, z)]^2$. The condition (11) corresponds to the lack of the initial fluctuation power beyond the Nyquist wavenumber $k_{\rm Nyquist} \sim k_{\rm max}$, while the condition (12) reflects the finite mass resolution corresponding to the simulation particles. In principle, the condition (12) also affects the halo-halo term, equation (8), however we do not include it, because our aim here is to extract the most essential feature considering the most important defect in the numerical simulation for each term. We have found, however, that including the correction results in only a minor change in the estimates for the P^{hh} term, so we do not consider the condition (12) in the halo-halo term below. Specifically, the dashed lines plotted in left and right panels of Figure 1 adopt $R_{\rm min} \equiv \pi/k_{\rm max} = 0.3$, 1, $3h^{-1}$Mpc, and $M_{\rm min} = 10^{11}h^{-1}M_\odot$, $3 \times 10^{11}h^{-1}M_\odot$, $10^{12}h^{-1}M_\odot$, from top to bottom.

The message from these plots is that the dark matter clustering below the mean separation length is really sensitive to the two parameters $k_{\rm max}$ and $M_{\rm min}$. In particular, the effect is quite substantial at higher redshifts where the major fraction of mass is contained in less massive halos that cannot be resolved with a given particle mass in simulations. In the next section we compare our model predictions with the evolution of simulation data.

3. COMPARISON WITH n-BODY DATA

3.1. *N-body data*

For the present purpose, we need the current best simulation data. So we decided to use VIRGO-SCDM and VIRGO-ΛCDM simulations (Jenkins et al. 1998) and HUBBLE-ΛCDM (Jenkins et al. 2001; Evrard et al. 2001), all of which are publicly available. The simulation parameters are summarized in Table 1. Their initial conditions were generated using the CDM transfer functions computed by Bond & Efstathiou (1984) for the VIRGO simulations, while CMBFAST (Seljak & Zaldarriaga 1996) is used for the Hubble volume simulation which is well approximated by the analytic fitting function by Eisenstein & Hu (1998). For the VIRGO simulations, we use snapshot data at $z = 1$, 2 and 3 for SCDM, and at $z = 1$, 3 and 5 for ΛCDM. In the case of the Hubble volume ΛCDM simulation, we do not use the full snapshot data at z, but rather "deep wedge" light-cone output. This dataset subtends an 81.45 square-degree field from its apex (a fiducial observer position) at a corner of the simulation box directed along a diagonal of the simulation box up to $z = 4.9$ (Hamana et al. 2001b)[3]. From this light-cone output, we generate

[3] For details of the output formats of the Hubble volume simulation, see the Hubble volume project home page: http://www.mpa-garching.mpg.de/Virgo/hubble.html

TABLE 1
PARAMETERS ADOPTED IN THE SIMULATION MODELS.

	$\Omega_{\rm m}$	Ω_Λ	$\Omega_{\rm b}$	h	σ_8	$N_{\rm part}$	$z_{\rm init}$	$m_{\rm part}$ $(h^{-1}M_\odot)$	$\lambda_{\rm part}$ $(h^{-1}{\rm Mpc})$	$\epsilon_{\rm grav}$ $(h^{-1}{\rm Mpc})$
VIRGO-SCDM	1.0	0.0	0.0	0.5	0.51	256^3	50	2.27×10^{11}	0.94	0.03
VIRGO-ΛCDM	0.3	0.7	0.0	0.7	0.9	256^3	30	6.86×10^{10}	0.94	0.03
HUBBLE-ΛCDM	0.3	0.7	0.04	0.7	0.9	10^9	35	2.22×10^{12}	3.0	0.1

three slice subsamples with depth of $200h^{-1}$Mpc centered at $z = 0.5$, 1.5 and 2.5.

We compute the two-point correlation function of dark matter particles using the pair-count estimator proposed by Landy & Szalay (1993):

$$\xi(r) = \frac{DD(r) - 2DR(r) + RR(r)}{RR(r)}. \qquad (13)$$

In so doing, we distribute the same number of random particles as simulation particles for each model.

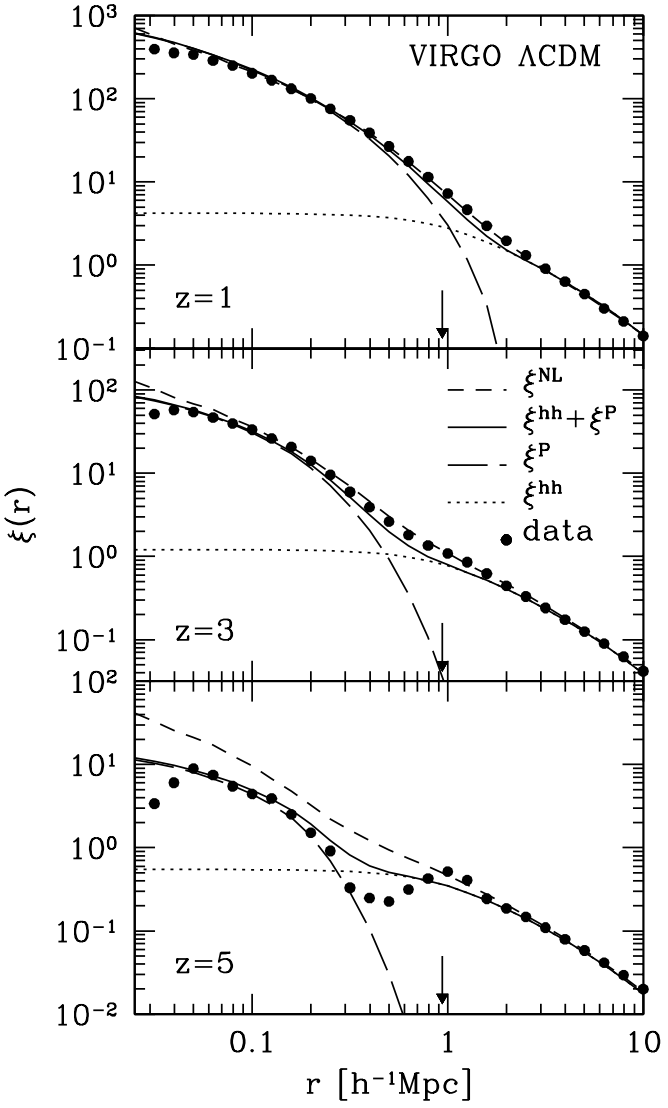


FIG. 3.— Same as Fig. 2 but for VIRGO-ΛCDM simulation.

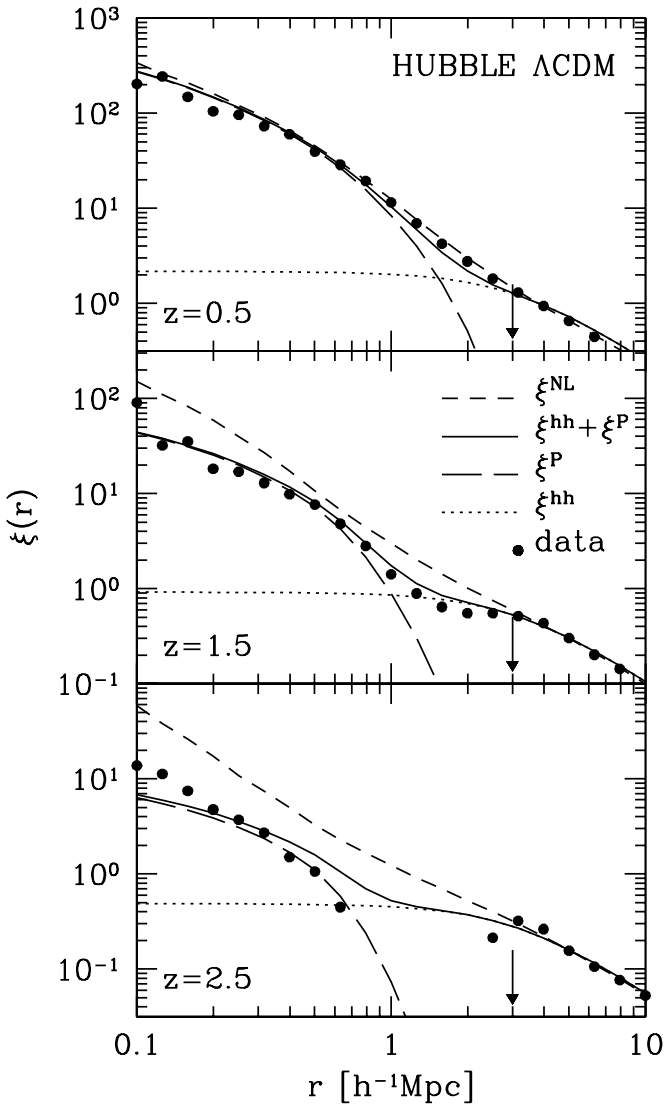


FIG. 4.— Same as Fig. 2 but for Hubble volume ΛCDM simulation.

3.2. *Model predictions*

We compute model predictions on the basis of the dark halo approach which take into account the limitations due to the lack of the initial fluctuation power and the finite mass resolution by introducing the two parameters $k_{\rm max}$ and $M_{\rm min}$ as described in §2.3. For definiteness we set $k_{\rm max}$ as $k_{\rm Nyquist} = \pi/\lambda_{\rm part}$ for each simulation. The minimum mass scale whose density profile can be resolved in simulations is determined by the particle mass $m_{\rm part}$, but the precise value is somewhat uncertain. In the analysis below we use $M_{\rm min} = \mu m_{\rm part}$ with $\mu = 4$, which, we find, reasonably fits the N-body data almost independently of

either the redshift or simulation parameters.

3.3. *Evolution of the dark matter clustering at $r < \lambda_{\rm part}$*

Figures 2 to 4 present the comparison between the simulation data and our model predictions for Virgo SCDM, Virgo ΛCDM and Hubble ΛCDM data at different redshifts. The filled circles show the two-point correlation functions measured directly from each simulation output. The mean separation lengths $\lambda_{\rm part}$ of simulation particles are indicated by arrows. Dashed lines show the nonlinear prediction by Peacock & Dodds (1996). Predictions by the dark halo approach, to which corrections for the lack of small-scale perturbation power and the finite particle mass are made (see §2), are shown by dotted, long-dashed and solid lines for the halo-halo term, Poisson term and their sum, respectively. It is important to keep in mind that the fitting function by Peacock & Dodds (1996) may have 10 to 20 percent uncertainty depending on the cosmological model and scale (Peacock & Dodds 1996), thus a small disagreement found at very small scales in lower redshift cases may be partly due to a failure of the fitting formula (Jenkins et al. 1998).

At $r > \lambda_{\rm part}$, the halo-halo term almost perfectly reproduces the simulation results. This reflects the fact that the evolution of large-scale structure is insensitive on average to the details of the smaller-scale clustering; incidentally this is why we can safely apply linear theory on large scales without specifying the small-scale inhomogeneity.

The evolution of clustering at $r < \lambda_{\rm part}$ is more interesting. On these scales, one cannot assign the proper amplitude of fluctuation spectra predicted from linear theory at $z_{\rm init}$. Nevertheless at $z = (3-5)$, the almost right amount of power has been already generated by the nonlinear mode-coupling from the larger scales. This suggests that the rate of the nonlinear power transfer is sufficiently rapid. As a result, at those epochs the small-scale power in simulations is primarily limited by the finite mass resolution rather than the lack of the initial fluctuation power on the corresponding scales.

3.4. *When can we trust the small-scale dark matter clustering in simulations ?*

It is remarkable that the two-point correlation function in simulations on scales below the mean particle separation does not seriously suffer from the lack of the initial fluctuation power, at least at later epochs. Nevertheless the resulting dark matter clustering is still below the nonlinear prediction due to the finite mass resolution which cannot be accounted within the 10 to 20 percent uncertainty in the nonlinear fitting formula (Peacock & Dodds 1996; Jenkins et al. 1998). In fact, this systematic introduces error in the computed correlation function for simulations with lower mass resolution and/or at higher redshifts. Then one might naturally ask when the small-scale dark matter clustering in simulations becomes reliable. We propose an empirical criterion as follows.

We have already shown that the small-scale dark matter clustering is primarily limited by the finite mass resolution. Also the Poisson term would be dominated by halos which become nonlinear at that epoch. The characteristic mass for gravitationally collapsed objects, $M_{\rm NL}(z)$, is approximately given by the condition $\sigma(M_{\rm NL}, z) = 1$. Therefore this mass scale should be much larger than the simulation particle mass $m_{\rm part}$ so as to reproduce the proper amplitude of the Poisson term.

Since the small-scale dark matter clustering mainly comes from the Poisson term (§2), the absence of halos with a mass comparable to and less than the particle mass in a N-body simulation leads to a lack of the clustering amplitude at small scales. Therefore, in order to reproduce the proper amplitude of the Poisson term at a certain time, halos with at least a characteristic mass for gravitationally collapsed objects at that time must be resolved. Such characteristic mass, $M_{\rm NL}(z)$, is approximately given by the condition $\sigma(M_{\rm NL}, z) = 1$, and should be much larger than the simulation particle mass $m_{\rm part}$ so as to be resolved in a N-body simulation. This requirement can be translated to the criterion for the critical redshift $z_{\rm crit}$ when simulations reasonably resolve the dark matter clustering on scales below the mean separation:

$$M_{\rm NL}(z_{\rm crit}) = n_{\rm halo} m_{\rm part}. \tag{14}$$

In the above we introduce a fudge factor $n_{\rm halo}$ so as to represent the number of particles that is required to reasonably resolve a single halo of the nonlinear mass. Usually $n_{\rm halo}$ is typically supposed to be around 10, but, as far as statistical measures such as the dark matter two-point correlation functions are concerned, it could be much smaller; we used $n_{\rm halo} \sim \mu = 4$ in plotting Figures 2 to 4, for instance.

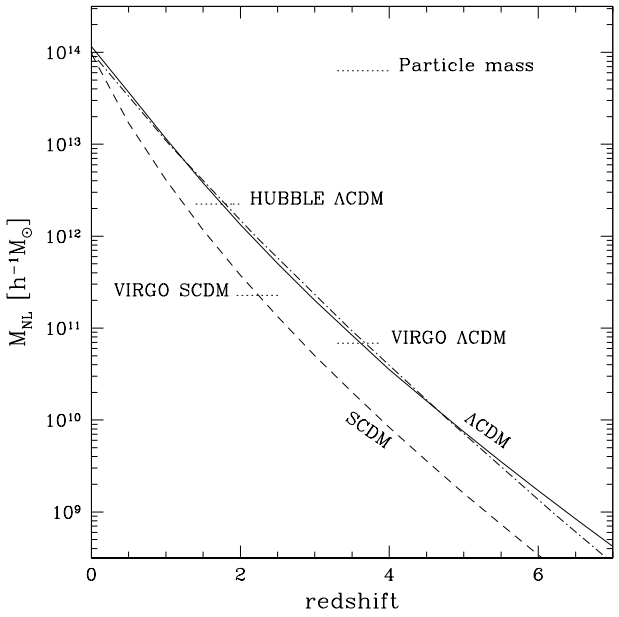


FIG. 5.— The nonlinear mass scale $M_{\rm NL}$ defined by $\sigma_R(M_{\rm NL}) = 1$ versus redshift. The solid and dashed lines are for ΛCDM and SCDM model, respectively. The dotted horizontal lines shows the particle masses of N-body simulations used in §3. The dot-dashed line shows the fitting function of $M_{\rm NL}$-$z_{\rm crit}$ relation for ΛCDM model, equation (15).

In Figure 5, we plot $M_{\rm NL}(z)$ against redshift for the SCDM (dashed lines) and ΛCDM (solid lines) parameters of the present simulations. The particle masses for the three simulation models are marked in dotted lines. The dot-dashed line shows the approximate relation for

the ΛCDM model that fits the relation for the ΛCDM model within 10 percent accuracy for $0 < z < 6$;

$$z_{\rm crit} = 0.72 \left[\log_{10} \left(\frac{2 \times 10^{15} h^{-1} M_\odot}{n_{\rm halo} m_{\rm part}} \right) \right]^{1.25} - 1. \quad (15)$$

As far as the dark matter correlations on scales below the mean particle separation are concerned, one should not trust the simulation data at $z > z_{\rm crit}$. It is important to note that this criterion does *not* mean all results from such N-body simulations are unreliable, but should be applied only to the dark matter correlations at small scales.

4. SUMMARY AND DISCUSSION

We have examined the reliability of dark matter correlation in cosmological high-resolution N-body simulations on scales below the mean particle separation. The particle discreteness effect imposes two fundamental limitations on those scales; the lack of initial fluctuation power and finite mass resolution. We applied dark halo approach to discuss separately how these two limitations affect the simulation results at later epochs. We found that nonlinear power transfer below the mean particle separation (up to the force resolution) is sufficiently rapid that the reliability of the simulations is primarily determined by the mass of particles. By a detailed comparison with three major cosmological simulations, we conclude that at $z > z_{\rm crit}$ the small scale dark matter correlations in high-resolution N-body simulations are not reliable. Of course it is impossible to *prove* that the opposite is true at $z < z_{\rm crit}$. Nevertheless our comparison indicates also that the small scale dark matter clustering in a high-resolution N-body simulation is reliable down to the gravitational force resolution length for $z < z_{\rm crit}$ at least as far as the two-point correlation functions are concerned. It must be noted that this criterion does *not* mean that all results from such N-body simulations are unreliable. The limitation of the reliability of a measurement from N-body simulations depends on the quantity one wants to examine.

The criterion should be applied only to measurements of the dark matter clustering such as its two-point correlation function and power spectrum. Splinter et al. (1998) concluded that phase sensitive statistics exhibit strongly the effect of discreteness. Strictly speaking our conclusion is not inconsistent with their finding, because the two-point correlation is insensitive to the phase information and the difference would largely come from the higher-order correlations that we do not attempt to compare. In principle our model could be generalized to higher-order correlations, but there is no reliable empirical model for those statistics that we can test against, to the quantitative degree of the Peacock-Dodds prediction for the two-point correlation function.

We believe that the present methodology to test the reliability of the dark matter clustering in a numerical simulation is original and powerful, and at least complementary to a more traditional way of searching for the convergence among different numerical codes with different resolutions. On the other hand, we have to note that these approaches are not completely independent; the major ingredients in our model "predictions" including the nonlinear mass power spectrum (Peacock & Dodds 1996), the mass function of halos (Sheth & Tormen 1999), and the density profile of halos (Navarro, Frenk & White 1996) are actually *calibrated* by high-resolution simulations. We have assumed that those calibrations are performed by *perfect* simulations, applied the resulting *predictions* to the current problem, and found that our model remarkably reproduces what we measure from simulation data. The present methodology may still suffer from some calibration uncertainties. Part of this difficulty is already illustrated in the small but systematic deviation of our predictions and simulation data on scales one-order-of magnitude smaller than the mean separation. Most likely this is due to the gravitational softening effect in simulation data. Nevertheless it is also true that the model prediction in those scales may be sensitive to the choice of the inner slope of halo profile; we adopted the NFW value, 1.0, throughout the paper, but it could be 1.5 as many recent simulations indicate (Fukushige & Makino 1997; Moore et al. 1998). Therefore we do not claim that the validity of the Peacock-Dodds prediction and our halo approach has been tested below those scales. Our conclusion, however, is valid on scales above ~ 0.1 times the mean separation lengths where those details are not critical.

Exactly for these reasons, we hope to revisit and reexamine the reliability of the model predictions calibrated by existing simulations in future.

We would like to thank Simon White for valuable comments and his careful reading of the manuscript, and Gerhard Börner for useful comments. T.H. thanks Matthias Bartelmann for the hospitality during his stay at MPA where most of the present work was performed. He also acknowledges support from Research Fellowships of the Japan Society for the Promotion of Science. The simulations used in this work were carried out by the Virgo Consortium and the data are publicly available at http://www.mpa-garching.mpg.de/NumCos. Numerical computation in the present work was partly carried out at the Yukawa Institute Computer Facility. This research was supported in part by the Grant-in-Aid by the Ministry of Education, Science, Sports and Culture of Japan (07CE2002, 12640231).

REFERENCES

Aarseth, S. J., Gott, J. R., & Turner, E. L. 1979, ApJ, 228, 664
Bahcall, N. A., & Cen, R. Y. 1993, ApJ, 407, L49
Bartelmann, M., Huss, A., Colberg, J., Jenkins, A., & Pearce, F. R. 1998, A&A, 330, 1
Bond, J. R., & Efstathiou, G. 1984, ApJ, 285, L45
Bullock, J. S., Kolatt, T. S., Sigad, Y., Somerville, R. S., Kravtsov, A. V., Klypin, A. A., Primack, J. R., & Dekel, A. 2001, MNRAS, 321, 559
Colberg, J. M. et al., (The Virgo Consortium) 2000, MNRAS, 319, 209
Cole, S., Aragón-Salamanca, A., Frenk, C., Navvaro, J., & Zept, S., 1994, MNRAS, 271, 781
Cole, S., Fisher, K. B., & Weinberg, D. H. 1994, MNRAS, 267, 785
Cooray, A., Hu, W., & Miralda-Escude, J. 2000, ApJ, 535, L9
Cooray, A., & Hu, W. 2000, ApJ, 548, 7
Davis, M., Efstathiou, G., Frenk, C. S., & White, S. D. M. 1985, ApJ, 292, 371
Efstathiou, G., Davis, M., Frenk, C. S., & White, S. D. M. 1985, ApJS, 57, 241

Efstathiou, G., Frenk, C. S., White, S. D. M., & Davis, M. 1988, MNRAS, 235, 715
Eisenstein, D. J., & Hu, W. 1998, ApJ, 496, 605
Evrard, A. E. et al. 2001, ApJ, submitted (astro-ph/0110246)
Fukushige, T., & Makino, J. 1997, ApJ, 477, L9
Gelb, J. M., & Bertschinger, E. 1994, ApJ, 436, 467
Hamana, T., Colombi, S., & Suto, Y. 2001a, A&A, 367, 18
Hamana, T., Yoshida, N., Suto, Y., & Evrard, A. E. 2001b, ApJ, 561, L143
Hamilton, A. J. S., Kumar, P., Lu, E., & Matthews, A. 1991 ApJ, 374, L1
Henry, J. P. 2000, ApJ, 534, 565
Jenkins, A., et al., (The Virgo Consortium) 1998, ApJ, 499, 20
Jenkins, A., Frenk, C. S., White, S. D. M., Colberg, J. M., Cole, S., Evrard, A. E., Couchman, H. M. P., & Yoshida, N. 2001, MNRAS, 321, 372
Jing, Y. P. 1998, ApJ, 503, L9
Jing, Y. P., & Suto, Y. 1998, ApJ, 494, L5
Jing, Y. P., & Suto, Y. 2000, ApJ, 529, L69
Kauffmann, G., White, S. D. M., & Guiderdoni B. 1993, MNRAS, 264, 201
Kayo, I., Taruya, A., & Suto, Y. 2001, ApJ, 561, 22
Knebe, A., Kravtsov, A., Gottlöber, S., Klypin, A. 2000, MNRAS, 317, 630.
Kerscher, M., Szapudi, I., & Szalay, A. S. 2000, ApJ, 535, L13
Komatsu, E., & Kitayama, T. 1999, ApJ., 526, L1
Lacey, C., & Cole, S. 1993, MNRAS, 262, 627
Lahav, O., Itoh, M., Inagaki, S. & Suto, Y. 1993, ApJ, 402, 387
Landy, S. D., & Szalay, A. S. 1993, ApJ, 412, 64
Limber, D. N. 1953, ApJ, 117, 134
Ma, C.-P. & Fry, J. N. 2000, ApJ, 543, 503
McClelland, J., & Silk, J. 1977, ApJ, 217, 331
Magira, H., Jing, Y. P., & Suto, Y. 2000, ApJ, 528, 30
Makino, N., Sasaki, M., & Suto, Y. 1992, Phys. Rev. D, 46, 585
Matsubara, T., & Suto, Y. 1994, ApJ, 420, 497
Melott, A. L., Splinter, R. J., Shandarin, S. F., & Suto Y. 1997, ApJ, 479, L79
Miyoshi, K., & Kihara, T. 1975, PASJ, 27, 333
Mo, H. J., & White, S. D. M. 1996, MNRAS, 282, 347
Moore, B., Governato, F., Quinn, T., Stadel, J., & Lake, G. 1998, ApJ, 499, L5
Nakamura, T. T., & Suto, Y. 1997, Prog. Theor. Phys., 97, 49
Navarro, J., Frenk, C., & White, S. D. M. 1996, ApJ, 462, 563
Navarro, J., Frenk, C., & White, S. D. M. 1997, ApJ, 490, 493
Neyman, J., & Scott, E. L. 1952, ApJ, 116, 144
Peacock, J. A., & Dodds, S. J. 1996, MNRAS, 280, L19
Peacock, J. A., & Smith, R. E. 2000, MNRAS, 318, 1144
Peebles, P. J. E. 1974, A&A, 32, 197
Peebles, P. J. E. 1980, Large-Scale Structure of the Universe (Princeton: Princeton Univ. Press)
Press, W., & Schechter,, P. 1974, ApJ, 187, 425
Somerville, R. S., Lemson, G., Sigad, Y., Dekel, A., Kauffmann, G., & White, S. D. M. 2001, MNRAS, 320, 289
Somerville, R. S., & Primack, J. 1999, MNRAS, 310, 1087
Scherrer, R. J., & Bertschinger, E. 1991, ApJ, 381, 349
Seljak, U. 2000, MNRAS, 318, 203
Seljak, U., & Zaldarriaga, M. 1996, ApJ, 469, 437
Sheth, R. K., & Jain, B.. 1997, MNRAS, 285, 231
Sheth, R. K., & Tormen, G. 1999, MNRAS, 308, 119
Splinter, R. J., Melott, A. L., Shandarin, S. F., & Suto Y. 1998, ApJ, 497, 38
Suginohara, T., Suto, Y., Bouchet, F. R., & Hernquist, L. 1991, ApJS, 75, 631
Suto, Y., Itoh, M., & Inagaki, S. 1990, ApJ, 350, 492
Suto, Y., & Suginohara, T. 1991, ApJ, 370, L15
Suto, Y. 1993, Prog.Theo.Phys., 90, 1173
Suto, Y., & Matsubara, T. 1994, ApJ, 420, 504
Suto, Y., & Sasaki, M. 1991, Phys. Rev. Letters, 66, 264
Taruya, A., Magira, H., Jing, Y. P., & Suto, Y. 2001, PASJ, 53, 155
Taruya, A., & Suto, Y. 2000, ApJ, 542, 559
Watanabe, T., Matsubara, T., & Suto, Y. 1994, ApJ, 432, 17
White, S. D. M. 1996, in Cosmology and Large-Scale Structure, ed. R. Schaefer, J. Silk, M. Spiro, & J. Zinn-Justin (Dordrecht: Elsevier)
White, S. D. M., & Frenk, C. S., 1991, ApJ, 379, 52
Yoshida, N., Springel, V., White, S. D. M., & Tormen, G. 2000, ApJ, 544, L87